J Mol Model (2010) 16:965–974
DOI 10.1007/s00894-009-0603-1

ORIGINAL PAPER

Hydrogen bonding interactions in PN···HX complexes: DFT and ab initio studies of structure, properties and topology

Pradeep Risikrishna Varadwaj

Received: 7 August 2009 / Accepted: 29 September 2009 / Published online: 23 October 2009

Abstract Spin-restricted DFT (X3LYP and B3LYP) and ab initio (MP2(fc) and CCSD(fc)) calculations in conjunction with the Aug-CC-pVDZ and Aug-CC-pVTZ basis sets were performed on a series of hydrogen bonded complexes PN···HX (X = F, Cl, Br) to examine the variations of their equilibrium gas phase structures, energetic stabilities, electronic properties, and vibrational characteristics in their electronic ground states. In all cases the complexes were predicted to be stable with respect to the constituent monomers. The interaction energy (ΔE) calculated using a super-molecular model is found to be in this order: PN···HF > PN···HCl > PN···HBr in the series examined. Analysis of various physically meaningful contributions arising from the Kitaura-Morokuma (KM) and reduced variational space self-consistent-field (RVS-SCF) energy decomposition procedures shows that the electrostatic energy has significant contribution to the over-all interaction energy. Dipole moment enhancement ($\Delta\mu$) was observed in these complexes expected of predominant dipole-dipole electrostatic interaction and was found to follow the trend PN···HF > PN···HCl > PN···HBr at the CCSD level. However, the DFT (X3LYP and B3LYP) and MP2 levels less accurately determined these values (in this order HF < HCl < HBr). Examination of the harmonic vibrational modes reveals that the PN and HX bands exhibit characteristic blue- and red shifts with concomitant bond contraction and elongation, respectively, on hydrogen bond formation. The topological or critical point (CP) analysis using the static quantum theory of atoms in molecules (QTAIM) of Bader was considered to classify and to gain further insight into the nature of interaction existing in the monomers PN and HX, and between them on H-bond formation. It is found from the analysis of the electron density ρ_c, the Laplacian of electron charge density $\nabla^2\rho_c$, and the total energy density (H_c) at the critical points between the interatomic regions that the interaction N···H is indeed electrostatic in origin ($\rho_c>0$, $\nabla^2\rho_c>0$ and $H_c>0$ at the BCP) whilst the bonds in PN ($\rho_c>0$, $\nabla^2\rho_c>0$ and $H_c<0$) and HX (($\rho_c>0$, $\nabla^2\rho_c<0$ and $H_c<0$)) are predominantly covalent. A natural bond orbital (NBO) analysis of the second order perturbation energy lowering, $E^{(2)}$, caused by charge transfer mechanism shows that the interaction N···H is n(N) → BD*(HX) delocalization.

Keywords PN···HX complexes · Linear hydrogen bonding · Ab initio and DFT calculations · Electronic structures · Energy decomposition analysis · Vibrational properties · NBO analysis · Topological properties

P. R. Varadwaj (✉)
Department of Chemistry, Faculty of Sciences,
Okayama University,
Tsushima-naka 3-1-1, Okayama-Shi,
Okayama-ken 700-8530, Japan
e-mail: pradeep@t.okayama-u.ac.jp

Introduction

Numerous research articles have been devoted to the hydrogen-bonded and the van der Waals complexes not only for the understanding of the nature of interaction but also due to their importance in the construction of new materials with deterministic material properties [1, 2]. A great deal of complexes have been studied where hydrogen halides HX (X = F, Cl, Br) were considered as proton denoting subunits and nitrogen N as the proton-accepting atomic center, and are of the types N···HX, where X is an element with an electronegativity greater than H. The HF containing complexes result in larger interaction energy because of its larger dipole moment compared to the

complexes containing other halogen halides [1–5]. Of the most important characteristic properties, it has been established that the conventional H-bonded interactions undergo the electronic structure change of the proton accepting and denoting molecules, the red-shift of the HX harmonic vibrational frequency, the enhancement of the HX IR band intensity, the HOMO to LUMO charge transfer, and the electric dipole moment enhancement [1–8]. The quantitative spectroscopic measure of these observed effects are decreasing in trend with respect to the increasing size of the hydrogen halides in the complex (for a given proton acceptor molecule) [4, 5].

Molecular phosphorous nitride (P≡N) is one of the most widespread and abundant phosphorous bearing species detected in the interstellar medium in the gas phase [9, 10]. It has received a considerable amount of attention not only due to its coordination chemistry with transition metal cations in forming capped octahedron (β-cages) complexes [11, 12] and their importance as an insulating coating material for semi-conductor surfaces [13] but also due to the lack of understanding of energetics of the controversial gas phase endothermic reaction ½ P_2+1/2 N_2 = PN [14].

PN is a highly polar diatomic molecule (μ=2.7 D) and its electron-donor capacity can be evaluated related to its concurrent capacity to participate in hydrogen bonding as a proton acceptor. Ahlrichs et al. [14] have shown, at the SCF level of theory, that PN forms stable dimeric and trimetric complexes. The trimeric complex, $(PN)_3$, is energetically preferable (D_{3h} point group symmetry) over the dimeric form (not yet experimentally observed); the former being planar ring-shaped in its structural arrangement in the gas phase. The CPF and SCF ab initio calculations [14, 15] and the experimental IR spectroscopy of $(PN)_3$ have been reported elsewhere [16].

Recently, a computational study of CH_2CHOH^{2+} + PN has been performed to explore the proton-transfer reactivity of CH_2CHOH^{2+} [17]. Zhengfa et al. [18] have studied the resulting structural, vibrational, and energetic properties of the reaction between PH_2 and NO using ab initio and DFT levels. They have shown that the reaction results in PN and H_2O, and is strongly exothermic with a release of −189.6 kJ mol^{-1} of energy.

Attention has not yet been given to the complexes formed between PN and HX, however, studies on similar types of complexes, viz., N_2···HX (X = F, Cl, Br) [19–21] and CO···HX (X = F, Cl, Br) [22–24], have been largely carried out. Thus, the main purpose of this study was to investigate theoretically on the existence of hydrogen bonding interactions in the PN···HX series of complexes in the gas phase with a view to assess the energetic stability of the complexes formed; the monomers are small diatomic polar molecules: heteronuclear halogen halides HX (X = F, Cl, Br) as proton donors and PN as proton acceptor. Since the P and N ends of PN can be treated as proton accepting centers (expected of the presence of electron lone-pairs), there is a geometrical possibility of hydrogen bonding interactions of the types NP···HX, NP···XH, and PN···HX.

Ab initio and DFT methods are widely applied to complexes of similar types for a precise determination of various molecular electronic properties [25–27]. We, therefore, have studied the PN···HX (X = F, Cl, Br) complexes at the CCSD(fc) [28], MP2(fc) [29], and DFT (B3LYP [30, 31], X3LYP [27, 32]) levels in conjunction with the basis sets Aug-CC-pVDZ and Aug-CC-pVTZ to investigate variations in the hydrogen bonding properties. Note that the DFT functional X3LYP gives reasonable estimates of energetics of hydrogen bonded and van der Waals complexes including transition metal systems [27, 32–35] whilst the B3LYP functional underestimates for the same [36, 37].

In this communication, we report the computed structural properties, electronic properties, and characteristic harmonic vibrational frequencies of the linearly H-bonded PN···HX (X = F, Cl, Br) complexes. The binding energies of the complexes were evaluated using a super-molecular approach and analyzed in the series. Various physically meaningful contributions to the over-all interaction energy of the complexes arising mainly from electrostatic, exchange, polarization, and charge transfer effects were evaluated quantitatively on the X3LYP optimized geometries based on the Kitaura-Morokuma (KM) [38, 39] and the reduced variational space self-consistent-field (RVS-SCF) energy decomposition formalisms [40, 41], and the results are presented. The normal mode vibrational frequencies were assigned with confidence, and compared with conventional hydrogen bonded complexes of similar types. Since topological or critical point (CP) approach can yield a great deal of information, we have applied the quantum theory of atoms in molecules (QTAIM) of Bader [42] to these systems specifically to classify the types of bonding involved (close shell and/or open shell) in the monomers HX and PN, and between them on H-bond formation. Since QTAIM analysis does not provide origin of these interactions, the natural bond orbital analysis has been performed to estimate quantitatively the second order perturbation energy lowering $E^{(2)}$ caused by the charge transfer mechanism.

Computational details

Unless otherwise stated, all the electronic structure calculations were performed with the help of GAUSSIAN 03 [43], and WinGamess [44] suite of programs. Visualizations and normal mode analysis were performed with the help of MacMolPlt [45].

Geometries of the monomers and the complexes were optimized at the X3LYP [27, 32] and B3LYP [30, 31] levels of theory in conjunction with the Aug-CC-pVTZ (ACCT) basis set using restricted spin formalism in their ground electronic states. The basis set ACCT is a correlation consistent polarized valence triple zeta of Dunning and co-workers [46, 47] augmented with d-functions on the heavy atoms. The X3LYP level calculations were performed using WinGamess [44] since this functional was inaccessible with the present version of GAUSSIAN 03 [43]. For reasons to be discussed later, we have also optimized the geometries of the complexes and the monomers at the MP2(fc)/ACCT (with MP2 density) [29] and CCSD (fc)/Aug-CC-pVDZ levels [28] (with QCI/CC density) using the frozen-core approximation. We have performed Hessian calculations following each of the energy-minimized structures to characterize the nature of the stationary point; absence of imaginary harmonic frequencies in the resulting output files confirm that the structures obtained are genuine minima and are corresponding to the C∝υ point group symmetry. The frequency shifts ($\Delta\omega$) were then approximated by the relation $\Delta\omega = \omega^{\text{complex}} - \omega^{\text{monomer}}$.

The binding (or stabilization or interaction) energy (ΔE) of these complexes was calculated using a super-molecular approach [48] without and incorporating zero-point vibrational energy (ZPVE) given by Eqs. 1 and 2.

$$\Delta E = E^{PN\cdots HF} - \left(E^{PN} + E^{HX}\right), \quad (1)$$

$$\Delta E^{c} = -\Delta E - ZPVE^{PN\cdots HF} + \left(ZPVE^{PN} + ZPVE^{HX}\right), \quad (2)$$

where E represents the total energy. Since this procedure is known to be susceptible of basis set superposition error (BSSE) while using a finite size basis set, we corrected for BSSE using the commonly used counterpoise procedure of Boys and Bernardi [49] at the CCSD/Aug-CC-pVDZ level. We did not perform BSSE correction at other levels since it is unnecessary to go for a BBSE correction when using Aug-CC-pVTZ basis set [50], and that it has a tendency to overcorrect for the interaction energy at the MP2 level [26].

We have carried out energy decomposition analysis (EDA) using the Kitaura-Morokuma (KM) [38, 39] and the reduced variational space self-consistent-field (RVS-SCF) [40, 41] schemes. According to the KM energy decomposition formalism, the interaction energy of an inter-molecular complex is defined as

$$\Delta E = E_{ES} + E_{PL} + E_{EX} + E_{CT} + E_{MIX}, \quad (3)$$

where E_{ES} is the electrostatic energy, E_{PL} is the energy of polarization, E_{EX} is the energy of exchange repulsion, E_{CT} is the energy of charge transfer or electron delocalization, and E_{MIX} is the coupling energy. In addition, there are other terms that account for the BSSE, and finally, E_{RES} covers residual terms of energy.

On the other hand, the RVS approach is defined within the HF-SCF framework and is an extension of the KM scheme. According to this model, HF interaction energies are deconvoluted into four separate local contributions given by Eq. 4.

$$\Delta E = (E_{EL} + E_{EX}) + E_{PL} + E_{CT}, \quad (4)$$

where the terms on the right hand side have a similar meaning as in the KM approach. For the estimation of the components in Eqs. 3 and 4, we have applied the GAMESS implementation [44] of the RHF level to the optimized X3LYP geometries of the complexes.

The natural bond orbital (NBO) analysis has been applied successfully to a number of hydrogen bonded systems [51–54]. It has been demonstrated that the NBO results [53] and the values of most of the properties from a topological analysis of the electron charge density [55] are sensitive to the imbalance of basis sets. The NBO results obtained using the Dunning-type correlation consistent basis sets exhibit much weaker basis set dependent than those using the Pople basis sets [56]. We, therefore, carried out NBO analysis at the CCSD/Aug-CC-pVDZ level. The wavefunctions were analyzed using the NBO 3.0 set of programs [57, 58] available in GAUSSIAN 03. The molecular electrostatic potentials on the surfaces of N and H atoms of the monomers and the complexes were evaluated at the same level using GAUSSIAN 03 since they are particularly suited for the analysis of non-covalent interactions.

The topological parameters at the bond critical points (BCPs) of the monomers and the complexes were evaluated at the CCSD/Aug-CC-pVDZ level based on Bader's QTAIM theory [42] using AIMALL suite of programs [59].

Results and discussion

Monomers

Table 1 summarizes the key computed property parameters of the monomers. These consist of the inter-nuclear bond distances (*R*), the harmonic vibrational frequencies (ω), the molecular dipole moments (μ), the entropies (*S*), and the zero-point vibrational energies (ZPVE). Included are also the available experimental data [60] for comparison.

The X3LYP values of the bond distances of the monomers are close to the experimental values whilst the B3LYP values slightly overestimate these bond distances except for PN. The CCSD(fc) and MP2(fc) methods give

Table 1 Key property[a] parameters of the monomers HX (X = F, Cl, Br) and PN obtained from various levels of theory

Monomer	Method	Basis[b]	R(Å)	ω (cm^{-1})	μ(D)	S(J/mol–K)	ZPVE($kJmol^{-1}$)
HF	X3LYP	ACCT	0.9231	4112	1.810	173.59	24.60
	B3LYP	ACCT	0.9241	4072	1.812	173.61	24.36
	MP2(fc)	ACCT	0.9218	4123	1.810	173.57	24.66
	CCSD(fc)	ACCD	0.9221	4117	1.810	173.57	24.63
	Expt [60]		0.9168	4138	1.820	173.78	24.75
HCl	X3LYP	ACCT	1.2808	2972	1.095	186.55	17.78
	B3LYP	ACCT	1.2837	2942	1.116	186.59	17.60
	MP2(fc)	ACCT	1.2747	3044	1.115	186.47	18.21
	CCSD(fc)	ACCD	1.2906	2989	1.159	186.68	17.88
	Expt [60]		1.2746	2991	1.080	186.90	17.89
HBr	X3LYP	ACCT	1.4244	2649	0.840	198.40	15.79
	B3LYP	ACCT	1.4249	2618	0.837	198.41	15.66
	MP2(fc)	ACCT	1.4066	2762	0.860	198.20	16.52
	CCSD(fc)	ACCD	1.4247	2682	0.887	198.41	16.04
	Expt [60]		1.4144	2649	0.827	198.59	15.84
PN	X3LYP	ACCT	1.4811	1406	2.929	210.84	8.41
	B3LYP	ACCT	1.4879	1400	2.870	110.92	8.38
	MP2(fc)	ACCT	1.5293	1179	2.602	211.48	7.05
	CCSD(fc)	ACCD	1.5145	1329	2.760	211.24	7.95
	Expt [60]		1.4909	1337	2.751	211.13	7.998

[a] R is the equilibrium bond length, ω is the HX harmonic vibrational frequency, μ is the dipole moment, S is the entropy, and ZPVE is the zero-point vibrational energy

[b] ACCD and ACCT refer the Aug-CC-pVDZ and Aug-CC-pVTZ basis sets, respectively

the best estimate of the bond lengths for HX; however they largely overestimate for the PN bond length by 0.0236 and 0.0384 Å, respectively.

The experimental values of the harmonic vibrational frequencies and the molecular dipole moments of the monomers are well reproduced. The scaling factors (theor./expt.) obtained for the harmonic vibrational frequencies (0.97–1.0) are typical for DFT methods [61–63]; however, the performance of the X3LYP level is better than the B3LYP and MP2 levels; deviations are as small as 26, 19, 0 and 69 cm^{-1} at the X3LYP/ACCT level, 66, 49, 31, and 63 cm^{-1} at the B3LYP/ACCT level, and are as large as 15, 53, 113, and 158 cm^{-1} at the MP2/ACCT level for HF, HCl, HBr, and PN, respectively. The CCSD level gives the best estimates of these values. The B3LYP and X3LYP values of entropy are in agreement with each other and compare well with the experimental values while the MP2 level underestimates for the halogen halides and overestimates for PN. Moreover, the X3LYP and CCSD levels give good estimate of ZPVEs whilst the MP2 level slightly overestimates for the same for HX and underestimates largely (~1 kJ mol^{-1}) for PN when compared against the experimental value. In conclusion, the overall performance of the X3LYP functional is reasonably good and agrees well with those obtained from the CCSD level. Nevertheless, it is encouraging that the bond lengths are all reproduced within 0.04 Å, the dipole moments within 0.05 D, the entropies within 0.5 $Jmol^{-1}K^{-1}$, and the ZPVEs within 1 kJ mol^{-1}.

Complexes

Geometries and structural changes

The results of this calculation for the equilibrium properties of the complexes PN···HX (X = F, Cl, Br) are summarized in Table 2. For the interaction between PN and HX is considered to be a hydrogen bond, two necessary conditions must be satisfied. Firstly, the H atom must be shared between two electronegative atoms with the H-atom covalently bonded to one of them. This is indeed the case here, N and F are two electronegative atoms and the H atom is covalently bonded to X = F, Cl, Br). Secondly, the geometrical criterion should be such that the hydrogen bond distance (in this case, N···H bond distance) must be less than the sum of the van der Waals radii of atoms involved directly (in this case, N and H) in the H-bond formation. The N···H bond distances are computed to be in the range from 1.7689 to 1.8629 Å for PN···HF, from 1.9454 to 2.0667 Å for PN···HCl, and from 1.9628 to 2.1372 Å PN···HBr irrespective of the correlated methods. These distances are all less than the sum of van der Waals radii of N (1.55 Å [64]) and H atoms (1.20 Å [65], and the value recommended by the Cambridge Crystallographic Database is 1.09 Å [64]), and are ordered in the series as: PN···HF < PN···HCl < PN···HBr, indicating that HF forms the strongest hydrogen bond with PN compared to the other proton donors.

The interaction between PN and HX results in the PN bond contraction and the HX bond elongation. A measure of the

Table 2 Key property[a] parameters of the PN···HX (X = F, Cl, Br) complexes obtained from various levels of theory

Monomer	Method	Basis[b]	R(N···H)/Å	Δ_g(HX)/Å	Δ_g(PN)/Å	Δμ/D	ΔE/kJ mol^{-1}	ZPVE/(kJmol^{-1})	ΔE^c/(kJmol^{-1})
PN···HF	X3LYP	ACCT	1.7689	0.0199	0.0042	1.475	−39.21	41.40	30.82
	B3LYP	ACCT	1.7808	0.0213	0.0041	1.458	−36.50	40.82	28.42
	MP2(fc)	ACCT	1.8117	0.0177	0.0050	1.299	−36.44	39.81	28.34
	CCSD(fc)	ACCD	1.8629	0.0137	0.0042	1.240	−33.64	40.61	25.60(−29.72)
PN···HCl	X3LYP	ACCT	1.9657	0.0155	0.0027	1.492	−22.76	31.96	16.99
	B3LYP	ACCT	1.9753	0.0157	0.0026	1.473	−20.93	31.47	15.42
	MP2(fc)	ACCT	1.9454	0.0144	0.0029	1.369	−26.58	30.86	20.98
	CCSD(fc)	ACCD	2.0667	0.0081	0.0026	1.193	−22.26	31.38	16.71(−18.64)
PN···HBr	X3LYP	ACCT	2.0146	0.0133	0.0024	1.564	−19.04	29.36	13.88
	B3LYP	ACCT	2.0386	0.0151	0.0022	1.505	−16.96	28.78	12.22
	MP2(fc)	ACCT	1.9628	0.0132	0.0024	1.470	−25.74	28.59	20.73
	CCSD(fc)	ACCD	2.1372	0.0060	0.0020	1.178	−19.53	28.85	14.67(−15.43)

[a] R is the H-bond length, Δ_g is the geometrical parameter [25], Δμ is the dipole moment enhancement, ΔE is the uncorrected binding energy (Eq. 1), and ΔE^c is the zero-point corrected energy (Eq. 2) of the complex. Values in the parenthesis are the BSSE corrected energy, ΔE^c (BSSE)

[b] ACCD and ACCT refer the Aug-CC-pVDZ and Aug-CC-pVTZ basis sets, respectively

H-bond strength can be realized in view of the geometrical parameter defined by $\Delta_g(\mathrm{HX}) = \left(\mathrm{HX}^{\mathrm{complex}} - \mathrm{HX}^{\mathrm{free}}\right)/\mathrm{HX}^{\mathrm{free}}$, where free and complex refer, respectively, the HX bond distances when they are isolated and in the complexes [25]. The Δ_g value is computed to be the highest (~0.014 Å) for PN···HF and the least (~0.006 Å) for PN···HBr at the CCSD level. A similar trend is also evident for the geometrical parameter of PN, Δ_g(PN), when passing from HF through HBr in the series.

Energetic stability

The uncorrected interaction energy (ΔE) of a complex is calculated by differentiating between the total energy of the complex and sum of the total energies of the monomers given by Eq. 1. As can be seen from Table 2, all the correlated methods predict that the complexes are stable over the constituent monomers. The B3LYP ΔE values are 2.71 kJ mol^{-1} (for PN···HF), 1.83 kJ mol^{-1} (for PN···HCl), and 2.08 kJ mol^{-1} (for PN···HBr) smaller than the X3LYP values. The MP2 method significantly overestimates the interaction energies of PN···HCl and PN···HBr compared to the CCSD and X3LYP values whilst the B3LYP level underestimates for the same. The underestimation can be interpreted due to the fact that the energies resulting from weak interactions such as dispersion is largely missing at the DFT-B3LYP level whilst the other correlated levels account it for. Nevertheless, all the correlated methods predict the energetic stability of the complexes in this order: PN···HF > PN···HCl > PN···HBr. The uncorrected interaction energy reduces (on average) by ~8.3 kJ mol^{-1} for PN···HF, ~5.8 kJ mol^{-1} for PN···HCl, and ~5.1 kJ mol^{-1} for PN···HBr by incorporating the zero-point vibrational energy correction. Inclusion of the BSSE correction at the CCSD level leads the uncorrected H-bond energy reduced by 3.9 kJ mol^{-1} for PN···HF, 3.6 kJ mol^{-1} for PN···HCl, and 4.1 kJ mol^{-1} for PN···HBr.

Further analysis has been carried out to gain information about physically meaningful energetic contributions since hydrogen-bonding interaction is thought to arise from electrostatic, polarization, and charge transfer components. Since the X3LYP level predicts reasonable values of the bond lengths and the other physical parameters compared to the CCSD level, we have performed the KM [38, 39] and the RVS-SCF [40, 41] EDA analyses on the X3LYP/Aug-CC-pVTZ equilibrium structures. The results are summarized in Table 3. Based on the RVS-SCF energy decomposition analysis, the CT effect contributes the least (10.84 kJ mol^{-1} for PN···HF, 8.03 kJ mol^{-1} for PN···HCl, and 7.61 kJ mol^{-1} for PN···HBr) among all the energy terms whilst the electrostatic component is significant (57.91 kJ mol^{-1} for PN···HF, 39.29 kJ mol^{-1} for PN···HCl and 35.35 kJ mol^{-1} for PN···HBr). For comparison, the KM scheme yields virtually similar values of electrostatic and exchange components since these two terms are identical in the two approaches. However, it unusually predicts large E_{PL} and E_{CT} values compared to the RVS-SCF scheme. This known problem is basically due to the large mixing term that significantly increases the polarization and CT energies in the KM analysis because of the violation of Pauli exclusion principle.

The BSSE corrected energies, ΔE(BSSE), obtained from the EDA are in agreement with the zero-pointed corrected

Table 3 Computed energy components[a] of the PN···HX (X = F, Cl, Br) complexes (in kJ mol^{-1}) obtained from the RVS and the KM analyses at the RHF/Aug-CC-pVTZ level on the RX3LYP/Aug-CC-pVTZ energy-minimized structures. The upper and lower lines represent, respectively, the RVS and KM values

Complex	E_{ES}	E_{EX}	$E_{ES} + E_{EX}$	E_{PL}	E_{CT}	E_{MIX}	$E_{ES} + E_X + E_{PL} + E_{CT}$	ΔE	BSSE	ΔE(BSSE)
PN…HF	−57.91	54.39	−3.52	−15.56	−10.84	—	−29.92	−31.59	0.38	−31.21
	−57.91	54.39	−3.52	−32.74	−16.84	21.51	−53.10	−31.59	0.54	−31.05
PN…HCl	−39.29	43.14	3.85	−9.16	−8.03	—	−13.35	−14.52	0.21	−14.31
	−39.29	43.14	3.85	−19.71	−18.24	19.58	−34.10	−14.52	0.29	−14.23
PN…HBr	−35.35	41.92	6.57	−8.66	−7.61	—	−9.71	−10.79	0.25	−10.59
	−35.35	41.92	6.57	−19.75	−18.07	20.46	−31.25	−10.79	0.29	−10.50

[a] E_{ES} is the electrostatic energy, E_{EX} is the energy of exchange repulsion, E_{PL} is the energy of polarization, E_{CT} is the energy of charge transfer or electron delocalization, E_{MIX} is the coupling energy, ΔE is the H-bond energy, and ΔE(BSSE) is the BSSE corrected H-bond energy

binding energies (ΔE^c) of the corresponding complexes; deviations between them are ~0.4, 2.7, and 3.3 kJ mol^{-1} for the complexes containing HF, HCl, and HBr, respectively. This deviation is expected since the energy decomposition schemes are purely RHF based and therefore, they do not incorporate dispersion energy contributions expected of genuine hydrogen bonded systems.

Vibrational analysis

The association of PN with HX originates three new modes of vibration, viz., the N···H stretching vibration (ω_σ) and two doubly degenerate bending vibrations (ω_A and ω_D). The N···H stretching vibration is predicted below 200 cm^{-1}, the bending vibration of the proton acceptor molecule (ω_A) is below 100 cm^{-1} whilst of the proton donor molecules (ω_D) is above 350 cm^{-1} within the series examined (see Table 4, values are reported only at the highest level). This observation is in agreement with the experimental frequencies of similar type of complexes. For instance, the reported values of ω_A and ω_D are, respectively, 59.2 [19] and 271 cm^{-1} [66] for N_2···HF, 75 [22] and 348 cm^{-1} [67] for CO···HF, 73.6 and 550 cm^{-1} for HCN···HF [68], 9.1 [69] and 313 cm^{-1} [67] for CO_2···HF, and 45 [70] and 620 [71] cm^{-1} for CH_3CN···HF. The newly originated frequencies show a decreasing pattern with increasing size of HX (similar to the trend found for the binding energies of the complexes) in the series.

Arguing for the presence of a hydrogen bond is a red shift in the HF stretch of 293 cm^{-1} in PN···HF, the HCl stretch of 139 cm^{-1} in PN···HCl, and the HBr stretch of 97 cm^{-1} in PN···HBr. The observed trend in the HX band frequency is in agreement with the previously reported B3LYP/6-311++G(3df,3pd) results of PCCN···HX (339 cm^{-1} for HF, 171 cm^{-1} for HCl, and 117 cm^{-1} for HBr) [4] and ONCCN···HX (291 cm^{-1} for HF, 137 cm^{-1} HCl, and 85 cm^{-1} for HBr) complexes [5]. Moreover, it is also observed that the PN stretching frequency undergoes a blue-shift of 34, 20 and 16 cm^{-1}, respectively, for the complexes containing HF, HCl and HBr (expected of a 1:1 hydrogen bonded complex [72]). The red- and blue shifts parallel with the lengthening of the HX bond and the shortening of the PN bond, respectively.

Electronic properties

The charge transfer is often presumed to occur when the monomers find themselves in the proximity of each other [57]. The reason for this observed effect is due to the rearrangement of atomic charges on H-bond formation. For instance, the partial atomic charges computed (at the CCSD/Aug-CC-pVDZ level) using the natural population

Table 4 Computed CCSD(fc)/Aug-CC-pVDZ level inter-molecular harmonic vibrational frequencies[a] of the PN···HX (X = F, Cl, Br) complexes. Included are also the blue- and red-shifts calculated using the relation $\Delta\omega = \omega^{complex} - \omega^{monomer}$, where ω is the wave number and are given in units of cm^{-1}

Monomer	$\Delta\omega$(PN)	ω_σ (N···H)	$\Delta\omega$(HX)	ω_D(N···H)	ω_A(N···H)
PN…HF	34	166	−293	649	70
PN…HCl	20	104	−139	422	49
PN…HBr	16	79	−97	363	44

[a] ω_D and ω_A are the intermolecular degenerate bending vibrational modes of the proton donor and the proton acceptor molecules, respectively. ω_σ is the inter-molecular stretching mode.

analysis (NPA) show that the charge of H atom increases whilst that of N atom decreases upon complex formation. The charge on the H atom increased by 0.025*e* for PN···HF, 0.033*e* for PN···HCl and 0.036*e* for PN···HBr. This result is in consonant with the Bader's population analysis (see Table 5 for Q^H).

The charge rearrangement upon hydrogen bond formation results in the electric dipole moment enhancement ($\Delta\mu$) that stabilizes these complexes. $\Delta\mu$ is calculated by differentiating between the total dipole moment of the complex and the sum of the total dipole moments of the monomers (see Table 2). The B3LYP, X3LYP and MP2 levels computed $\Delta\mu$ values are found to agree with each other, and are ordered as PN···HF < PN···HCl < PN···HBr in the series. This ordering is in contrast with the computed binding energies of the complexes. Since DFT methods alone would not be convincing and that DFT is known to have problems with the representation of dispersion in weakly intermolecular interactions [24, 25, 51, 52], we extended our calculation at the CCSD(fc)/Aug-CC-pVDZ level. Encouragingly, the dipole moment enhancement parallels with the BSSE corrected H-bond energy at this level. It should be understood from this that the choice of an appropriate correlated method would certainly lead to the physically meaningful results for complexes of the type studied here.

Moreover, it has been established that the molecular electrostatic potential of proton acceptor or donor atoms can be used as reactive descriptors for the hydrogen bonding process [73, 74]. In the present systems, the electrostatic potential on the surface of the H-atom (V^H) becomes less negative (compared to the isolated molecules) whilst it becomes more negative on the surface of the N-atom (V^N) on hydrogen bond formation. The changes in the absolute values of V^H (compared to the isolated molecules) are 0.0499, 0.0278, and 0.0227 au while of V^N are 0.0264, 0.0201, and 0.0179 au upon the formation of PN···HF, PN···HCl, and PN···HBr, respectively (see Table 5). The trend in the changes of these values is in a direction similar to the order of interaction energies in the series.

Since the NBO theory describes the formation of these complexes caused by an inter-molecular charge transfer from the N atom lone-pair, *n*(N), of the idealized Lewis structure into the empty *anti*-bonding orbital BD*(HX), we carried out NBO analysis to assess *n*(N) → BD*(HX) delocalization that can be quantified by the second order perturbative estimates of $E^{(2)}$. $E^{(2)}\left(E^{(2)} = \Delta E_{ij} = q_i F(i,j)^2/\left(\varepsilon_i - \varepsilon_j\right)\right)$ is associated with the deloralization $i \rightarrow j$ where q_i is the donor orbital

Table 5 The electronic and topological properties[a,b] obtained from the CCSD(fc)/Aug-CC-pVDZ level calculations

Type	ρ_c	$\nabla 2\rho_c$	V_c	G_c	$\lvert V_c\rvert/G_c$	H_c	Q^H	E_b	$E^{(2)}$	V^H	V^N
Monomers											
PN	0.2119	1.4932	−0.6383	0.5058	1.2619	−0.1325					−18.3330
HF	0.3597	−3.0007	−0.9435	0.0966	9.7623	−0.8468	0.714			−0.9016	
HCl	0.2399	−0.8138	−0.3254	0.0610	5.3380	−0.2644	0.249			−0.9297	
HBr	0.1948	−0.3451	−0.2497	0.0817	3.0559	−0.1680	0.037			−0.9403	
Complexes											
PN….HF											
PN	0.2129	1.5276	−0.6461	0.5140	1.256997	−0.1321					
N…H	0.0287	0.1142	−0.0197	0.0241	0.816651	0.0044	0.730	25.86	14.02	−0.9515	−18.3066
HF	0.3388	−2.9492	−0.9201	0.0914	10.06697	−0.8287					
PN…HCl											
PN	0.2125	1.5145	−0.6432	0.5109	1.258932	−0.1323					
N…H	0.0210	0.0630	−0.0128	0.0143	0.897059	0.0015	0.335	16.82	11.28	−0.9575	−18.3129
HCl	0.2350	−0.8532	−0.3184	0.0526	6.05721	−0.2659					
PN….HBr											
PN	0.2124	1.5097	−0.6420	0.5097	1.259577	−0.1323					
N…H	0.0187	0.0530	−0.0111	0.0122	0.912546	0.0011	0.116	14.59	9.59	−0.9630	−18.3151
HBr	0.1941	−0.3935	−0.2381	0.0699	3.408102	−0.1683					

[a] Electron charge density (ρ_c), the Laplacian of charge density ($\nabla^2\rho_c$), the potential energy density (V_c), the kinetic energy density (G_c), the ratio $|V_c|/G_c$, the total energy density ($H_c=G_c+V_c$), Bader charge on H atom (Q^H/e), the stabilization energy (E_b/ kJ mol^{-1}) obtained from the relationship $E_b=(1/2)\,V_c$ [80], the second order perturbation energy lowering ($E^{(2)}$/kcal mol^{-1}) caused by charge transfer mechanism obtained from a NBO analysis, and the molecular electrostatic potentials (V^H and V^N, in au) at the N- and H-atoms of the isolated molecules and the complexes.

[b] Topological parameters are given in units of au. 1 au of ρ_c=6.7483 e Å^{-3}, 1 au of $\nabla^2\rho_c$=24.099 e Å^{-5}, 1 au of V_c, G_c, and H_c= 627.5095 kcal mol^{-1}

occupancy, F(i,j) is the off diagonal NBO Fock matrix element, ε_i and ε_j are the diagonal elements representing the orbital energies, and *i,j* represents donor NBO(i) and acceptor NBO(j), respectively. The value of $E^{(2)}$ for the *n* (N) → BD*(HX) delocalization is found to be the highest (14.02 kcal mol^{-1}) for PN···HF, 11.28 kcal mol^{-1} for PN···HCl, and the lowest (9.59 kcal mol^{-1}) for PN···HBr (see Table 5). The $E^{(2)}$ values correlate exponentially with the red-shift of the HX stretching vibration (see Fig. 1) demonstrating that $E^{(2)}$ can be used as a measure of the hydrogen bond strength. A similar relationship we have recently explored between $E^{(2)}$ and the O···H bond distances in a series of three amino-alcohol ligands [52].

Topological analysis

According to the Bader's QTAIM theory [42], the distinct interatomic interactions display characteristic features of electron charge density, ρ, at the (3, −1) critical point (CP). A necessary condition for a bond is that there must exist a (3, −1) CP in the inter-atomic region with electron density, ρ_c (c refers BCP), such that the path connecting between them, the so-called bond path, defines the unique axis of the BCP and the two atoms share an interatomic surface. The Laplacian of electron charge density $\nabla^2\rho_c$ determines the nature of the (3, −1) CP whether it is shared or close shell or a mixed interaction. For a predominantly covalent ("shared") interaction, ρ_c is usually >0.1 au and $\nabla^2\rho_c<0$ [75] ($\nabla^2\rho_c>0$ for highly polar bonds [76]), and for a predominantly ionic interaction ("closed shell"), the value of ρ_c is usually small (~10^{-2}au for a H-bond and ~10^{-3}au for a van der Waals interaction [75]) and $\nabla^2\rho_c>0$. At the boundary where $\nabla^2\rho_c=0$, the interaction is mixed in nature.

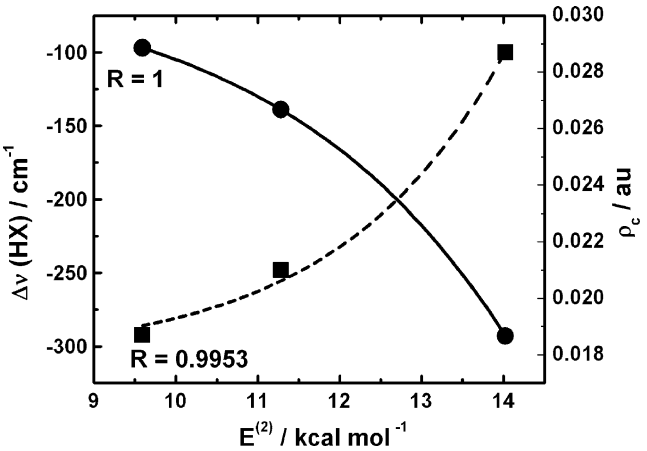

Fig. 1 Dependence of the second order perturbation lowering energy ($E^{(2)}$) caused by charge transfer between the N-atom lone-pair (n(N)) and the H–X *anti*-bonding orbitals (BD*(HX)) (**a**) with the red-shift of the HX stretches (Δω, •), and (**b**) with the electron charge density at the N···H BCPs (ρ_c, ■) of the PN···HX complexes. The data were fitted with an exponential function

First of all, Table 5 shows that ρ_c decreases at the HX BCPs passing from F through Br in the series. This indicates that the longer bonds correspond to a smaller accumulation of ρ_c at the BCP. Of all the monomers studied, ρ_c values are in this order: HF > HCl > PN > HBr. An examination of the Laplacian values at the BCP suggests that the bonds in hydrogen halides are predominantly covalent, and that the covalency decreases with a partial gain of ionic character with increasing size of the halogen atoms in HX. However, the value of $\nabla^2\rho_c$ at the P–N BCP is found to be positive. The reason for this observation is that the bond between P and N is largely polar due to the electronegative difference between the two atoms (3.04 for N and 2.19 for P on the Pauling scale). Therefore, it associates $\nabla^2\rho_c>0$ with a high ρ_c value indicating both a substantial accumulation of ρ_c near the inter-atomic surface and a transfer of ρ_c to the N atomic basin resulting in concentration there and depletion in the other. Similar results were reported previously for carbon oxides and carbon sulfides [42].

Upon the hydrogen bond formation, the magnitude of ρ_c values decreases at the HX BCPs whilst their values increase at the PN BCP. This electronic change is in agreement with the concomitant lengthening and shortening of the corresponding bonds, respectively. At the N···H BCP there is a small accumulation of ρ_c; values are 0.0287, 0.0210, and 0. 0187 au for PN···HF, PN···HCl, and PN···HBr, respectively. Figure 1 shows an exponential correlation of $E^{(2)}$ with ρ_c.

The $\nabla^2\rho_c$ value exhibits a decreasing order of charge concentration among the halogen halides in this order: HF > HCl > HBr irrespective of whether we consider isolated halogen halides or their association in the complex. The smaller values of ρ_c at the BCP is consistent with the fact that the Pauli exclusion principle operates to remove electron density from the interatomic surface resulting in a positive Laplacian and low electron density at the BCP [77]. The magnitudes of ρ_c ($\rho_c<0.10$) together with the sign of $\nabla^2\rho_c$ ($\nabla^2\rho_c>0$) at the N···H bond BCP are collectively indicative of a closed-shell interaction [42, 75–78].

Moreover, the sign of $\nabla^2\rho_c$ together with the values of ρ_c at BCP is not sufficient to characterize an interaction. Cremer and Kraka [79], therefore, have considered the total energy density, H_c, which is the sum of the local electron potential (V_c) and kinetic energy (G_c) densities, as an indicator of a bonded interaction by its sign and magnitude. Espinosa et al. [80] have established a correlation of the H-bond energy with the pressure exerted on the electrons around the critical point $V(r_c)$ given by the relation $E_b=1/2\ |V(r_c)|$. The estimated values of E_b are 25.86 (for PN···HF), 16.82 (for PN···HCl), and 14.59 kJ mol^{-1} (for PN···HBr). Interestingly, these values parallel with the binding energies of the complexes.

Jenkins and Morrison [81] and subsequently Espinosa et al. [82] have suggested using the ratio $|V_c|/G_c$ to characterize a bond. Interactions with $|V_c|/G_c<1$ and $H_c>0$ are characteristic of closed shell interactions (electrostatic); those with $|V_c|/G_c>2$ and $H_c<-G_c$ are typically open-shell interactions; and those with $1<|V_c|/G_c<2$ and $-G_c < H_c<0$ are diagnostic of interactions stabilized by local concentration of the charge of intermediate character. In the studied systems, the ratio $|V_c|/G_c$ ranges from 3 to 10 indicating that the H–X bond in the monomers and the complexes are predominantly covalent in character. The value of $|V_c|/G_c$ (~1.26, satisfy the condition $1<|V_c|/G_c<2$) along with H_c (~0.13 au) shows that the bond P–N is of intermediate character whilst the ratio $|V_c|/G_c<1$ (values range between 0.8–0.9) and $H_c>0$ at the N···H BCPs clarifies the close-shell nature of the interaction. The results are in consistent with the observations made by Nakanishi et al. [83] where they have reported that for hydrogen bonding $0.01<\rho_c<0.04$, $0.04<\nabla^2\rho_c<0.12$, and $-0.004<H_c<0.002$ au.

Conclusions

In this paper, we have studied theoretically the linear complexes of PN···HX (∠N···H–X=180°), which were formed by considering the nitrogen end of phosphorous nitride PN as the proton accepting molecular center and the halogen halides HX (X = F, Cl, Br) as proton donors. The correlated methods B3LYP, X3LYP, MP2(*fc*), and CCSD (*fc*) in conjunction with the basis sets Aug-CC-pVDZ and Aug-CC-pVTZ were applied to determine various physical parameters with a view to investigate the accuracy of the selected correlated levels and to investigate complex stability upon formation. All the correlated methods successfully reproduce experimental values of the monomers; however, the over-all performance of the CCSD level is better.

The predicted binding energies of the complexes are ordered as: PN···HF > PN···HCl > PN···HBr. The B3LYP functional underestimate the interaction energy significantly for PN···HCl and PN···HBr whilst the MP2 method overestimates for the same compared to the CCSD level. The BSSE and the zero-point vibrational energy corrections reduce the interaction energies as expected. Nevertheless, the H-bond energy values are typical for moderate hydrogen bonds (energies are in the range 12–60 kJ mol^{-1} and H-bond distances are in the range 1.5–2.5 angstrom [1]). The energy components derived from the KM and the RVS-SCF schemes indicate that the interaction between PN and HX is predominantly electrostatic, and that the polarization and charge transfer contribution to over-all interaction energy, ΔE, cannot be neglected. The energetic preference of the complexes in the series is in consonant with the electronic structure change of the PN and HX subunits (see Δ_g values), the blue- and red shifts of the harmonic vibrational frequencies of the PN and HX stretching modes, and the appearance of inter-molecular vibrational modes. Our result shows that the complex formation is accompanied by the dipole moment enhancement ($\Delta\mu$) at all the levels of theory. The observed trend in the values of $\Delta\mu$ at the CCSD level is in this order: PN···HF > PN···HCl >PN···HBr, however, the DFT (X3LYP and B3LYP) and MP2 levels incorrectly predict $\Delta\mu$ values in a reverse order.

Furthermore, a clear indication of the nature of bonding in the monomers and the complexes emerges from an explanation of various topological properties based on the Bader's QTAIM theory. From an analysis of the electron charge density, the Laplacian of charge density, and the energy densities it is found that $\rho_c>0$, $\nabla^2\rho_c<0$, $V_c<0$, $G_c>0$, $|V_c|/G_c>2$, and $H<0$ at the covalently shared HX BCPs, $\rho_c>0$, $\nabla^2\rho>0$, $1<|V_c|/G_c<2$, and $H_c<0$ at the PN BCP whilst $\rho_c>0$, $\nabla^2\rho_c>0$, $|V_c|/G_c<1$ and $H_c>0$ at the N···H BCP. The origin of the inter-molecular interaction between PN and HX has been explained by means of $n(N) \rightarrow BD^*(HX)$ delocalization and is quantified by the second order energy lowering $E^{(2)}$ caused by charge transfer. It is found that the $E^{(2)}$ values correlate with the red-shift of the HX stretches, and with the electron charge density, ρ_c, at the N···H BCPs of the complexes indicating that $E^{(2)}$ may be treated a measure of the hydrogen strength.

Acknowledgments PRV greatly acknowledges Japan Society for the Promotion of Science (JSPS) for the award of a Postdoctoral Fellowship and funding (Grant No: P 08349). The author thanks Prof. Sean A. C. McDowell and Prof. K. Kawaguchi for helpful discussions and rewarding supports. Thanks are due to the staffs of the Okayama University information science center for providing SX-6i supercomputing facility for GAUSSIAN 03 calculations.

References

1. Jeffrey GA (1997) An introduction to hydrogen bonding. Oxford Univ Press, New York
2. Scheiner S (1997) Hydrogen bonding: a theoretical perspective. Oxford University Press, US
3. Desiraju GR, Sreiner T (2003) The weak hydrogen bond. Oxford Univ Press, New York
4. Varadwaj PR, Husain MM (2006) Chem Phys Lett 424:227–232
5. Varadwaj PR (2007) Int J Quantum Chem 107:1194–1204
6. Rozenberg M, Loewenschuss A, Marcus Y (2000) Phys Chem Chem Phys 2:2699–2702
7. Ratajczak H (1972) J Phys Chem 76:3991–3992
8. Kemp DD, Gordon MS (2008) J Phys Chem A 112:4885–4894
9. Ziurys LM (1987) Astrophys J 321:L81–L85
10. The encyclopedia of Science. Available via DIALOG. http://www.daviddarling.info/encyclopedia/I/ismols.html
11. Schnick W, Lücke (1992) Angew Chem Int Ed Engl 31:213–215
12. Scherer OJ (1992) Angew Chem Int Ed Engl 31:170–171

13. Fukukawa Y, Mikami O, Okamura M, Hirota Y (1986) Proc Electrochem Soc 86:34 Also see via DIALOG. http://www.patentstorm.us/patents/6586318/description.html
14. Ahlrichs R, Bär M, Plitt HS, Schnöckel H (1989) Chem Phys Lett 161:179–184
15. Schnöckel H, Mehner T, Plitt HS, Schunck SC (1989) J Am Chem Soc 111:4578–4582
16. Atkins RM, Timms PL (1977) Spectrochim Acta Part A 33:853–857
17. Petrie S (2005) J Phys Chem A 109:6326–6334
18. Zhengfa HU, Zhenya W, Haiyang LI, Shikang Z (2002) Sci China A 45:1211–1218
19. Tang SN, Chuang CC, Mollaaghababa R, Klemperer W, Chang HC (1996) J Chem Phys 105:4385–4387
20. Mckellar ARW, Lu Z (1993) J Mol Spectrosc 161:542–551
21. Howard NW, Legon AC (1989) J Chem Phys 90:672–678
22. McMillen C, Bender D, Eliades M, Danzeiers D, Wofford BA, Bevan JB (1988) Chem Phys Lett 152:87–93
23. Soper PD, Legon AC, Flygare WH (1981) J Chem Phys 74:2138–2142
24. Legon AC, Soper PD, Keenan MR, Minton TK, Balle TJ, Flygare WH (1980) J Chem Phys 73:583–584
25. Grabowski SJ (2002) J Mol Struct 615:239–245
26. McDowell SAC (2006) Chem Phys Lett 424:239–242
27. Xu X, Goddard WA (2004) Proc Natl Acad Sci 101:2673
28. Scuseria GE, Schaefer HF III (1989) J Chem Phys 90:3700–3703
29. Møller C, Plesset MS (1934) Phys Rev 46:618–622
30. Becke AD (1988) J Chem Phys 88:1053–1062
31. Lee C, Yang W, Parr RG (1988) Phys Rev B 37:785–789
32. Xu X, Goddard WA (2004) J Phys Chem A 108:2305–2313
33. Xu X, Zhang Q, Muller RP, Goddard WA (2005) J Chem Phys 122:014105
34. Varadwaj PR, Cukrowki I, Marques HM (2008) J Phys Chem A 112:10657–10666
35. Varadwaj PR, Cukrowki I, Marques HM (2009) J Mol Struct Theochem 902:21–32
36. Tsuzuki S, Lüthi HP (2001) J Chem Phys 114:3949–3957
37. Rao L, Ke H, Xu X, Yan Y (2009) J Chem Theory Comput 5:86–96
38. Kitaura K, Morokuma K (1976) Int J Quantum Chem 10:325–340
39. Morokuma K, Kitaura K (1981) In: Politzer P, Truhlar DG (eds) Chemical applications of atomic and molecular electrostatic potentials. Plenum, New York, p 215
40. Bagus PS, Hermann K, Bauschlicher CW Jr (1984) J Chem Phys 80:4378–4386
41. Stevens WJ, Fink W (1987) Chem Phys Lett 139:15–22
42. Bader RFW (1990) Atoms in molecules: a quantum theory. Oxford University Press, Oxford
43. Frisch MJ et al (2004) GAUSSIAN 03, Revision C.02. Gaussian Inc, Pittsburg, PA
44. Schmidt MW, Baldridge KK, Boatz LA, Elbert ST, Gordon MS, Jensen JJ, Koseki S, Matsunaga N, Nguyen KA, Su S, Windus TL, Dupuis M, Montgomery JA (1993) J Comput Chem 14:1347–1363
45. MacMolPlt, version 7.2.1, Bode BM, Gordon MS (1998) J Mol Graphics Mod 16:133–138
46. Dunning TH Jr (1989) J Chem Phys 90:1007–1023
47. Kendall RA, Dunning TH Jr, Harrison RJ (1992) J Chem Phys 96:6796–6806
48. Pople JA (1982) Faraday Discuss Chem Soc 73:7–17
49. Boys SF, Bernardi F (1970) Mol Phys 19:553–566
50. Blanco F, Alkorta I, Solimannejad M, Elguero J (2009) J Phys Chem A 113:3237–3244
51. Wong NB, Cheung YS, Wu DY, Ren Y, Tian A, Li WK (2000) J Phys Chem A 104:6077–6082
52. Varadwaj PR, Cukrowski I, Marques HM (2009) DFT RX3LYP and RPBEPBE studies on the structural, electronic, and vibrational properties of some amino-alcohol ligands. Theochem. doi:10.1016/j.theochem.2009.08.009
53. Ludwig R (2000) J Mol Liq 84:65–75
54. Reed AE, Wienhold F, Curtiss LA, Pochatko DJ (1986) J Chem Phys 84:5687–5705
55. O'Brien SE, Popelier PLA (1999) Can J Chem 77:28–36
56. Goodman L, Sauers RR (2007) J Comput Chem 28:269–275
57. Weinhold F (1998) In: Schleyer PVR, Allinger ML, Clark T, Gasteiger J, Kollman PA, Schaefer HF, Schreiner PR (eds) Encyclopedia of computational chemistry, vol 3. John Wiley & Sons, Chichester, p 1792
58. Glendening EE, Reed AE, Carpenter JE, Weinhold F (2004) NBO 3.0, as implemented in GAUSSIAN 03, Revision C.02. Gaussian Inc, Pittsburg, PA
59. Keith TA (2008) AIMAll 08.05.04. Available via DIALOG. http://aim.tkgristmill.com
60. Computational Chemistry Comparison and Benchmark DataBase, NIST Standard Reference Database 101. Available via DIALOG. http://cccbdb.nist.gov/default.htm
61. Rauhut G, Pulay P (1995) J Am Chem Soc 117:4167–4172
62. Scott AP, Radom L (1996) J Phys Chem 100:16502–16513
63. Baker J, Jarzecki AA, Pulay P (1998) J Phys Chem A 102:1412
64. The Cambridge Structural Database, Radii & Bond lengths. Available via DIALOG. http://www.ccdc.cam.ac.uk/products/csd/radii/table.php4
65. Bondi A (1964) J Phys Chem 68:441–451
66. Goubet M, Asselin P, Manceron L, Soulard P, Perchard JP (2003) Phys Chem Chem Phys 5:3591–3594
67. Andrews L (1984) J Phys Chem 88:2940–2949
68. McIntosh A, Gallegos AM, Lucchese RR, Bevan JW (1997) J Chem Phys 107:8327–8337
69. Nesbitt DJ, Lovejoy CM (1992) J Chem Phys 96:5712–5725
70. Bevan JW, Legon AC, Millen DJ (1980) Proc R Soc Lond A 370:239
71. Legon AC, Millen DJ, North HM (1987) J Chem Phys 86:2530–2535
72. Pimentel GC, McClelland AL (1960) The hydrogen bond. Freeman, San Francisco, CA
73. Murray JS, Ranganathan S, Politzer P (1991) J Org Chem 56:3734–3737
74. Hagelin H, Murray JS, Brinck T, Berthelot M, Politzer P (1995) Can J Chem 73:483–488
75. Bader RFW, Essén H (1984) J Chem Phys 80:1943–1960
76. Bobrov MF, Popova GV, Tsirelson VG (2006) Russ J Phys Chem 80:584–590
77. Bader RFW (1998) J Phys Chem A 102:7314–7323
78. Bone RGA, Bader RFW (1996) J Phys Chem 100:10892–10911
79. Cremer D, Kraka E (1984) Angew Chem Int Ed Engl 23:627–628
80. Espinosa E, Molins E, Lecomte C (1998) Chem Phys Lett 285:170–173
81. Jenkins S, Morrison I (2000) Chem Phys Lett 317:97–102
82. Espinosa E, Alkorta I, Elguero J (2007) Euro J Chem Phys 117:5529
83. Nakanishi W, Hayashi S, Narahara K (2008) J Phys Chem A 112:13593–13599